Separating the causes of orbital ordering in $LaSr_2Mn_2O_7$ using resonant soft x-ray diffraction

2006 J. Phys.: Condens. Matter 18 L323

(http://iopscience.iop.org/0953-8984/18/24/L01)

INSTITUTE OF PHYSICS PUBLISHING JOURNAL OF PHYSICS: CONDENSED MATTER

J. Phys.: Condens. Matter **18** (2006) L323–L329 doi:10.1088/0953-8984/18/24/L01

LETTER TO THE EDITOR

Separating the causes of orbital ordering in $LaSr_2Mn_2O_7$ using resonant soft x-ray diffraction

S B Wilkins[1], N Stojić[2], T A W Beale[3], N Binggeli[2], P D Hatton[3], P Bencok[1], S Stanescu[1], J F Mitchell[4], P Abbamonte[5] and M Altarelli[2,6]

[1] European Synchrotron Radiation Facility, Boîte Postal 220, F-38043 Grenoble Cedex, France
[2] Abdus Salam International Centre for Theoretical Physics, Trieste 34014, Italy
[3] Department of Physics, University of Durham, Rochester Building, South Road, Durham DH1 3LE, UK
[4] Materials Science Division, Argonne National Laboratory, Argonne, IL 60439, USA
[5] National Synchrotron Light Source, Brookhaven National Laboratory, Upton, NY 11973, USA
[6] European XFEL Project Team, Desy, Notkerstraße 85, 22607 Hamburg, Germany

E-mail: wilkins@esrf.fr

Received 20 January 2006
Published 2 June 2006
Online at stacks.iop.org/JPhysCM/18/L323

Abstract

Resonant soft x-ray diffraction has been used to probe the temperature dependent orbital and magnetic structure of $LaSr_2Mn_2O_7$. Previous crystallographic studies have shown that this material has almost no MnO_6 oxygen displacements due to Jahn–Teller distortions at low temperatures. Within the low-temperature A-type antiferromagnetic phase, we found strong intensity at the $(\frac{1}{4}, \frac{1}{4}, 0)$ orbital and (0, 0, 1) magnetic reflections. This shows that even in the near absence of Jahn–Teller distortions, this compound is strongly orbitally ordered. A fit to the Mn L-edge resonance spectra demonstrates the presence of orbital ordering of the Mn^{3+} ions with virtually no Jahn–Teller crystal field in addition to possible Mn^{3+} and Mn^{2+}-like valence fluctuations.

(Some figures in this article are in colour only in the electronic version)

Ferromagnetism and charge ordering in the doped perovskite type manganese oxides $R_{1-x}A_xMnO_3$ (R = rare earth, A = Sr, Ca) have attracted considerable interest since the discovery of colossal magnetoresistance (CMR) [1]. Recently, much attention has been paid to the importance of the charge, lattice, spin and orbital degrees of freedom to explain the complex and anomalous structural, magnetic and transport behaviour observed in the manganites. The interplay between these degrees of freedom can cause localization of electrons on alternative manganese atoms to produce charge-ordered lattices. The ferromagnetism and metallic conductivity observed at low temperatures can be understood on the basis of the double-exchange mechanism, whereby e_g electrons hop between Mn sites through hybridization with

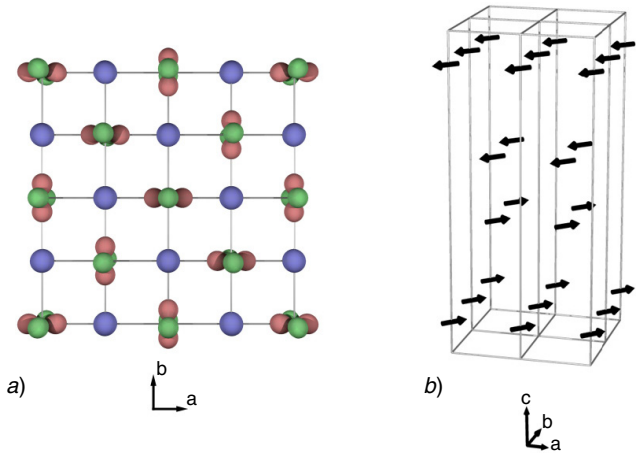

Figure 1. The crystal structure of the bilayer manganite $La_{2-2x}Sr_{1+2x}Mn_2O_7$ with $x = 0.5$ at low temperature. (a) The arrangement of the previously proposed 'Mn^{3+}' and 'Mn^{4+}' manganese ions are shown within the tetragonal unit cell. A plan view of the Mn^{3+} orbitals within the *ab* plane displaying orbital order of the $x^2 - z^2$, $y^2 - z^2$ type is given in (a). This is the dominant type of orbital ordering found in [18] for a doping $x = 0.42$. Our results suggest a chequerboard pattern closer to Mn^{2+}/Mn^{3+} rather than Mn^{3+}/Mn^{4+}; however, the alternating pattern remains the same. The arrangement of the magnetic spins of the Mn^{3+} ions in the low temperature antiferromagnetic structure is shown schematically in (b).

oxygen 2p orbitals and align the localized t_{2g} spins by strong Hund's coupling [2–4]. However, the understanding of the transport properties, such as CMR, and the complicated magnetic phase diagrams of the manganites requires a further ingredient, that of the orbital degree of freedom [5, 6].

The study of the orbital ordering phenomenon is, therefore, vital for the understanding of the complex properties of the manganite systems. Direct observation of orbital ordering in manganites has recently become possible using resonant soft x-ray diffraction at the Mn $L_{2,3}$ absorption edges after theoretical predictions by Castleton and Altarelli [7]. Mn $L_{2,3}$ resonant x-ray scattering experiments have been performed in $La_{0.5}Sr_{1.5}MnO_4$ [8, 9] and in $Pr_{0.6}Ca_{0.4}MnO_3$ [10]; however, in both cases the orbital degree of freedom is controlled by strong Jahn–Teller distortions. In this letter we report experimental results on $LaSr_2Mn_2O_7$. Previous crystallographic studies [11, 12] have indicated that this system undergoes extremely small Jahn–Teller distortions at low temperature. Despite this our results demonstrate the presence of long-range orbital order, in addition to magnetic order. The fit to the orbital ordering spectrum using multiplet calculations in a crystal field shows the presence of a vanishing Jahn–Teller distortion in addition to possible Mn^{3+} and Mn^{2+}-like valence fluctuations.

The samples were single crystals of the bilayer manganite $LaSr_2Mn_2O_7$, which were melt grown in flowing oxygen using a floating zone optical image furnace. The system $La_{2-2x}Sr_{1+2x}Mn_2O_7$ is a layered perovskite in which MnO_2 double layers and $(La, Sr)_2O_2$ blocking layers are stacked alternatively (see figure 1 from [12]). The reduced dimensionality causes the system to display a greatly enhanced magnetoresistance [13] and a reduced ferromagnetic transition temperature. Charge ordering has been reported in the temperature range from 100 to 200 K existing only over a narrow compositional range $0.475 < x < 0.55$ [14, 15]. Below 170 K the $x = 0.5$ material, $LaSr_2Mn_2O_7$, adopts an A-type antiferromagnetic ordering of the Mn spins [11] (see figure 1) and crystallographic and high-energy x-ray

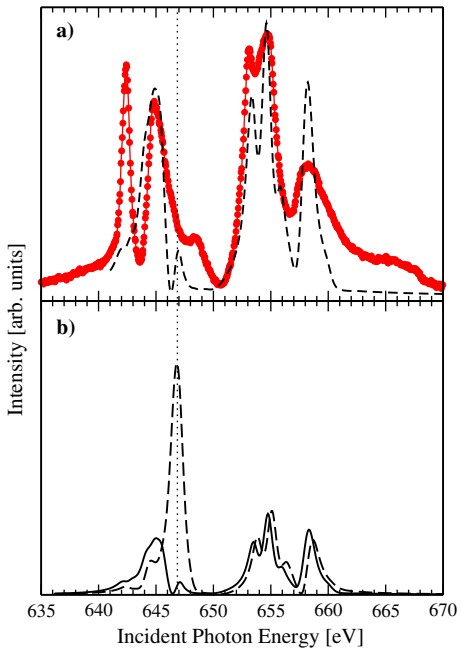

Figure 2. (a) Scattered x-ray intensity as a function of incident photon energy at constant wavevector $\vec{Q}_{OO} = (\frac{1}{4}, \frac{1}{4}, 0)$ (circles). The black dashed line shows the theoretical fit to the data. (b) Theoretical simulation (dashed black line) of the energy spectra with an eightfold increase in the Jahn–Teller distortion. The fit to the experimental data is repeated for comparison (solid line).

diffraction studies have shown the disappearance [11, 16] or reduction [17] of the Jahn–Teller distortion, such that the MnO_6 octahedra are almost undistorted below ∼100 K.

Experiments were carried out using the in-vacuum diffractometer on beamline ID08 at the European Synchrotron Radiation Facility. A single crystal of $LaSr_2Mn_2O_7$ cut with the [110] direction normal to the sample surface was used for measurements of the $(\frac{1}{4}, \frac{1}{4}, 0)$ orbital order reflection. Calibration of the energy of the incident x-ray beam at ID08 by gas absorption gives an absolute accuracy of 0.2 eV at 640 eV. Measurements of the anti-ferromagnetic reflection (001)were performed on a cleaved crystal with the [001] direction surface normal. The temperature dependences of both these reflections were obtained using beamline X1B at the National Synchrotron Light Source. At both beamlines the experimental procedure was identical to our previous studies [17, 8].

At ID08, the sample was cooled to ∼20 K using liquid helium and an intense and narrow reflection was found at a wavevector of $\vec{Q}_{OO} = (\frac{1}{4}, \frac{1}{4}, 0)$ at an incident energy of 643 eV. The solid circles in figure 2(a) show the scattered intensity as a function of the incident photon energy at constant wavevector, through the manganese L_3 and L_2 edges. On first inspection, there appear to be two main features at the L_3 edge and three at the L_2 edge. In contrast to previous measurements on $La_{0.5}Sr_{1.5}MnO_4$ [8] and $Pr_{0.6}Ca_{0.4}MnO_3$ [10] the maximum scattered intensity is primarily observed at the L_2 edge rather than at the L_3 edge. Measurements of the A-type antiferromagnetic reflection in $La_{2-2x}Sr_{1+2x}Mn_2O_7$ for $x = 0.475$ at $\vec{Q}_{AF} = (0, 0, 1)$ have been reported by Wilkins *et al* [17] at a temperature of 83 K. In figures 3(a) and (b) we show the scattered intensity measured at 20 K in $LaSr_2Mn_2O_7$ as a function of energy at constant wavevector. In this case, at the L_2 edge little scattering was

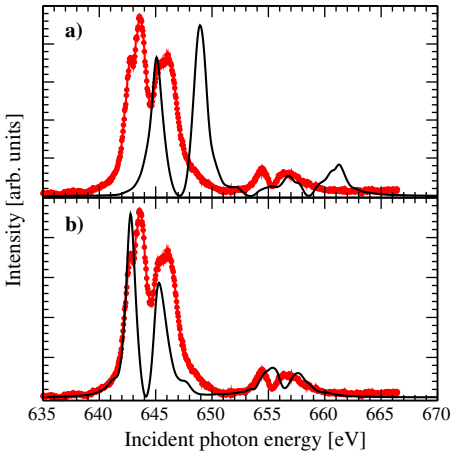

Figure 3. Scattered x-ray intensity as a function of incident photon energy at a constant wavevector $\vec{Q}_{\mathrm{AF}} = (0, 0, 1)$ (line with circles) with theoretical fits (solid black lines) describing the superposition of (a) Mn^{3+}/Mn^{4+} and (b) Mn^{3+}/Mn^{2+} type.

observed, but at the L_3 edge very strong intensity was found, which is comprised of two main features. Our experimental data in figures 2 and 3 indicate that $LaSr_2Mn_2O_7$ is simultaneously orbitally and magnetically ordered at low temperature. Soft x-ray diffraction is not particularly surface sensitive [17]. The inverse width in reciprocal space of the reflections gives an indication of the penetration depth. This indicates we are probing thousands of ångströms into the crystal.

In order to identify the origin of the resonant x-ray scattering signal, we have performed multiplet calculations in a crystal field. On the Mn^{3+} site with D_{4h} symmetry, two crystal field parameters are to be acquired from the fitting procedure: cubic (X^{400}) and tetragonal (X^{220}). In the absence of the experimental evidence, we assume that the spins are aligned in the [110] direction, which lowers the symmetry to that of the C_i point group. Choosing this direction as quantization axis, the resonant scattering amplitude at the orbital ordering wavevector $(\frac{1}{4}, \frac{1}{4}, 0)$ is proportional to the following combination of the atomic scattering tensors [19]:

$$f_{\mathrm{res}}^{\mathrm{OO}} \propto F_{0;1}^{\mathrm{e}} - F_{0;-1}^{\mathrm{e}} + F_{1;0}^{\mathrm{e}} - F_{-1;0}^{\mathrm{e}}, \tag{1}$$

with $F_{m;m'}^{\mathrm{e}}$ defined as

$$F_{m;m'}^{\mathrm{e}} = \sum_n \frac{\langle 0|J_m^{1\dagger}|n\rangle\langle n|J_{m'}^{1}|0\rangle}{E_0 - E_n + \hbar\omega + \mathrm{i}\Gamma/2}, \tag{2}$$

where m and m' denote polarization states and J_m^1 are the dipole operators defined in spherical coordinates. $|0\rangle$ represents the ground state with energy E_0 and $|n\rangle$ intermediate states with energy E_n. The photon energy is $\hbar\omega$ and Γ stands for the broadening due to the core–hole lifetime. Similarly, for the magnetic scattering with the wavevector (0, 0, 1), the scattering amplitude can be expressed as

$$f_{\mathrm{res}}^{\mathrm{MO}} \propto F_{1;1}^{\mathrm{e}} - F_{-1;-1}^{\mathrm{e}}. \tag{3}$$

The Slater integrals of the d–d and p–d direct and exchange interactions were scaled down to 75% of their atomic value. The p-shell spin–orbit parameter was increased by 9% from the Hartree–Fock value to correspond to the experimental value [20]. We used $\Gamma = 0.5$ eV for the

Lorentzian broadening due to the core–hole lifetime. In addition, to take into account also the experimental energy resolution, the scattering intensity, $I(\hbar\omega) \propto |f_{\rm res}|^2$, was convoluted with a Gaussian of width 0.1 eV.

The best fit to the orbital ordering is shown in figure 2(a). The corresponding crystal field parameters are $X^{400} = 3$ eV and $X^{220} = 0.4$ eV (or $10D_q = 0.91$ eV and $D_s = -0.048$ eV). The fit did not significantly change for variations of the cubic field X^{400} in the interval 3–4 eV and for the tetragonal (Jahn–Teller) field X^{220} in the interval 0.1–0.6 eV. The fit displays a fair general agreement with the experimental spectrum. The obtained L_3/L_2 ratio is satisfactory and we reproduce most of the structure from the experimental spectrum. However, the first peak in the L_3 edge is not reproduced[7] and broadened high-energy features at both edges are missing in the fit. These wide shoulders may be related to band-structure effects, which are not incorporated in our model. In figure 2(b) we illustrate the effect of an eightfold increase of the Jahn–Teller field. As shown before [21], the L_3/L_2 ratio is becoming larger with the increase in the tetragonal component of the crystal field. In our calculations a small Jahn–Teller tetragonal crystal field is necessary to lift the degeneracy of the e_g levels; however, the tetragonal field included is extremely small. Its value is one order of magnitude smaller than that obtained, e.g., for $La_{0.5}Sr_{1.5}MnO_4$ [21], so that, except for the lifting of orbital degeneracy, the Mn^{3+} ion is essentially in a cubic field. This shows we are within a regime where the scattering is dominated by orbital ordering of the e_g electrons.

We were not able to obtain a good fit to the magnetic scattering with Mn^{3+} ions alone, as it gave a single peak at each edge. Since $\vec{Q}_{\rm AF} = (0, 0, 1)$ sees a superposition of *all* manganese ions within the *ab* plane, we included an additional type of Mn ion in our model. Figure 3(a) shows the magnetic spectrum obtained by superposing the contributions of Mn^{3+} and Mn^{4+} with equal weights. The Mn^{4+} ion induces a peak at higher energy (at both edges) relative to the Mn^{3+} ion, as expected for ions with larger oxidation number [22]. This gives rise to a spectrum with two peaks at each edge, but shifted to a higher energy relative to the experimental spectrum. Moreover, the ratio between the two main features at both the L_3 and L_2 edges is inverted. In order to reproduce the feature at low energy, with a ratio consistent with experiment, we need to consider a Mn ion with lower oxidation number. In panel (b) of figure 3 we show the spectrum obtained with a 1:1 ratio of Mn^{2+} and Mn^{3+}. In these calculations, the Mn^{3+} crystal field parameters were taken to be exactly the same as for the orbital spectrum in figure 2(a), and the Mn^{2+} and Mn^{4+} spectra were calculated in a purely cubic crystal field ($X^{400} = 3.0$ eV). In figure 3, we positioned the Mn^{2+} (Mn^{4+}) edge, relative to the Mn^{3+} edge, using the theoretical chemical shifts obtained from our atomic multiplet calculations, i.e. ~ -2 and 4 eV, respectively. Experimental L-edge absorption results on Mn^{2+}, Mn^{3+}, and Mn^{4+} reference compounds show comparable chemical shifts (between -1 and -2 eV for Mn^{2+} and between 2 and 3 eV for Mn^{4+} [23–25]).

Surprisingly, much better agreement with the experimental data in figures 3(a) and (b) is obtained by the calculation for the Mn^{2+}/Mn^{3+} case than for the Mn^{3+}/Mn^{4+} case. This may simply reflect the basic limitations of the atomic multiplet calculations (which, for one thing, only allow integer values for the valence) to describe an extended system with non-negligible interatomic hopping; on the other hand, it is noteworthy that an average valence between 2+ and 3+ has recently been suggested by Hartree–Fock calculations [26, 27], and experimental data which indicate that the additional holes reside more on the oxygen ligands [28, 29]. Such a

[7] We were able to reproduce the first peak in the L_3 edge by increasing the cubic crystal field parameter. But, simultaneously, it was necessary to additionally significantly increase the 2p spin–orbit parameter. As such an increase could not be justified and is in contrast with results from [21], we do not present the corresponding fits. It should be noted, however, that even in this case the conclusion concerning the Jahn–Teller field remains: only a very small tetragonal field could reproduce the observed spectrum.

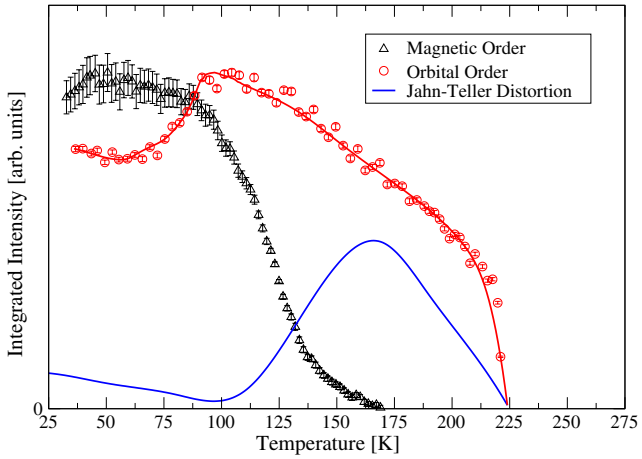

Figure 4. Temperature dependence of the integrated intensity of the $(\frac{1}{4}, \frac{1}{4}, 0)$ orbital order reflection and the (001)magnetic order reflection. The temperature dependence of the $(\frac{3}{4}, -\frac{1}{4}, 5)$ Jahn–Teller distortion peak, a measure of the amplitude of the Jahn–Teller distortion, is taken from [12].

change in the manganese valency from $3+/4+$ to $2+/3+$ would not alter the orbital occupancy of the Mn^{3+} ion. Both Mn^{2+} and Mn^{4+} are not Jahn–Teller active.

Figure 4 shows the temperature dependence of the orbital and magnetic reflections. The $(\frac{1}{4}, \frac{1}{4}, 0)$ reflection is observed below T_{OO}, which is coincident with T_{JT}. The Jahn–Teller distortions maximize at T_N ($\sim$170 K) and decrease below this temperature due to the occurrence of antiferromagnetic interactions. Note that the Jahn–Teller distortions are very weak below 100 K where the orbital and magnetic reflections are very strong. We note that below 100 K the Jahn–Teller distortions increase slightly, which coincides with a change in gradient of the intensity of the orbital and magnetic reflections.

In conclusion, we have reported the results of resonant soft x-ray scattering studies of the orbital and antiferromagnetic ordering in $LaSr_2Mn_2O_7$. The data of figures 2 and 3 immediately show that $LaSr_2Mn_2O_7$ is simultaneously both orbitally and antiferromagnetically ordered at low temperatures, despite the fact that the Jahn–Teller distortions in this system are measured to be very small. This is further supported by the theoretical fits, which display a good agreement with the experimental data for very small values of tetragonal crystal field. From these we can conclude that it is possible to obtain a strongly orbitally ordered phase within an A-type antiferromagnetic configuration in the absence of significant Jahn–Teller distortions. In such case, the energetics of the orbitally ordered configuration is favoured by the magnetic interactions, originating from the superexchange mechanism, as described by Goodenough [30]. The fit to the magnetic scattering data suggests a fluctuating valence situation, with Mn ions with valence charge between $+3$ and $+2$.

This work was supported by the Synchrotron Radiation Related Theory Network, SRRTN, of the EU. NS gratefully acknowledges the assistance of Paolo Carra in learning how to use the Cowan and 'Racah' codes. We thank F M F de Groot for helpful discussions. We are grateful for support from EPSRC for a studentship for TAWB and for a travel grant to NSLS.

References

[1] Jin S, Tiefel T H, McCormack M, Fastnacht R A, Ramesh R and Chen L H 1994 *Science* **264** 413
[2] Zener C 1951 *Phys. Rev.* **82** 403
[3] Anderson P W and Hasegawa H 1955 *Phys. Rev.* **100** 675
[4] de Gennes P G 1960 *Phys. Rev.* **118** 141
[5] Maezono R, Ishihara S and Nagaosa N 1998 *Phys. Rev.* B **58** 11583–96
[6] Mizokawa T and Fujimori A 1997 *Phys. Rev.* B **56** R493–6
[7] Castleton C W M and Altarelli M 2000 *Phys. Rev.* B **62** 1033–8
[8] Wilkins S B, Spencer P D, Hatton P D, Collins S P, Roper M D, Prabhakaran D and Boothroyd A T 2003 *Phys. Rev. Lett.* **91** 167205
[9] Dhesi S S, Mirone A, De Nadai C, Ohresser P, Bencok P, Brookes N B, Reutler P, Revcolevschi A, Tagliaferri A, Toulemonde O and van der Laan G 2004 *Phys. Rev. Lett.* **92** 056403
[10] Thomas K J, Hill J P, Grenier S, Kim Y-J, Abbamonte P, Venema L, Rusydi A, Tomioka Y, Tokura Y, McMorrow D F, Sawatzky G and van Veenendaal M 2004 *Phys. Rev. Lett.* **92** 237204
[11] Argyriou D N, Bordallo H N, Campbell B J, Cheetham A K, Cox D E, Gardner J S, Hanif K, dos Santos A and Strouse G F 2000 *Phys. Rev.* B **61** 15269–76
[12] Wilkins S B, Spencer P D, Beale T A W, Hatton P D, Zimmermann M V, Brown S D, Prabhakaran D and Boothroyd A T 2003 *Phys. Rev.* B **67** 205110
[13] Moritomo Y, Asamitsu A, Kuwahara H and Tokura Y 1996 *Nature* **380** 141
[14] Kimura T, Kumai R, Tokura Y, Li J Q and Matsui Y 1998 *Phys. Rev.* B **58** 11081–4
[15] Li J Q, Matsui Y, Kimura T and Tokura Y 1998 *Phys. Rev.* B **57** R3205–8
[16] Kubota M, Fujioka H, Hirota K, Ohoyama K, Moritomo Y, Yoshizawa H and Endoh Y 2000 *J. Phys. Soc. Japan* **69** 1606
[17] Wilkins S B, Hatton P D, Roper M D, Prabhakaran D and Boothroyd A T 2003 *Phys. Rev. Lett.* **90** 187201
[18] Koizumi A, Miyaki S, Kakutani Y, Koizumi H, Hiraoka N, Makoshi K, Sakai N, Hirota K and Murakami Y 2001 *Phys. Rev. Lett.* **86** 5589–92
[19] Stojić N, Binggeli N and Altarelli M 2005 *Phys. Rev.* B **72** 104108
[20] Thomson A *et al* 2001 *X-Ray Data Booklet* (Berkeley, CA: Lawrence Berkeley National Laboratory, University of California)
[21] Wilkins S B, Stojić N, Beale T A W, Binggeli N, Castleton C W M, Bencok P, Prabhakaran D, Boothroyd A T, Hatton P D and Altarelli M 2005 *Phys. Rev.* B **71** 245102
[22] Schofield P F, Henderson C M, Cressey G and van der Laan G 1995 *J. Synchrotron Radiat.* **2** 93
[23] Cramer S P, de Groot F M F, Ma Y, Chen C T, Sette F, Kipke C A, Eichhorn D M, Chan M K, Armstrong W H, Libby E, Christou G, Booker S, McKee V, Mullins O C and Fuggle J C 1991 *J. Am. Chem. Soc.* **113** 7937
[24] Morales F, de Groot F M F, Glatzel P, Kleimenov E, Bluhm H, Havecker M, Knop-Gericke A and Weckhuysen B M 2004 *J. Phys. Chem.* B **108** 16201
[25] Kobayashi S, Usui T, Ikuta H, Uchimoto Y and Wakihara M 2004 *J. Mater. Res.* **19** 2421
[26] Ferrari V, Towler M and Littlewood P B 2003 *Phys. Rev. Lett.* **91** 227202
[27] Zheng G and Patterson C H 2003 *Phys. Rev.* B **67** 220404
[28] Ju H L, Sohn H-C and Krishnan K M 1997 *Phys. Rev. Lett.* **79** 3230
[29] Subias G, Garcia J, Sanchez M C, Blasco J and Proietti M G 2002 *Surf. Rev. Lett.* **9** 1071
[30] Goodenough J B 1963 *Magnetism and the Chemical Bond* (New York: Interscience)